

ELECTRONIC SUPPLEMENTARY INFORMATION (E.S.I.)

Automated System for Extraction and Instantaneous Analysis of Millimeter-Sized Samples

Jie-Bi Hu,^a Ssu-Ying Chen,^a June-Tai Wu,^{b,c,d} Yu-Chie Chen,^{*a,e} Pawel L. Urban^{*a,e}

^a*Department of Applied Chemistry, National Chiao Tung University, Hsinchu, Taiwan*

^b*Institute of Molecular Medicine, College of Medicine, National Taiwan University, Taipei, Taiwan*

^c*Department of Medical Research, National Taiwan University Hospital, Taipei, Taiwan*

^d*Research Center for Developmental Biology and Regenerative Medicine, National Taiwan University, Taipei, Taiwan*

^e*Institute of Molecular Science, National Chiao Tung University, Hsinchu, Taiwan*

* Corresponding authors.

Fax +886-3-5723764

Calculation of the Reynolds number

Calculation of the Reynolds number (Re) was carried out according to the formula:

$$Re = \frac{\rho v L}{\mu}$$

where ρ is density of fluid (acetonitrile/water = 70:30 (v/v), $\sim 810 \text{ kg m}^{-3}$), v is the velocity of fluid ($\sim 0.011 \text{ m s}^{-1}$), L is the hydraulic diameter ($1.5 \times 10^{-4} \text{ m}$), and μ is the dynamic viscosity ($\sim 4.3 \times 10^{-4} \text{ Pa s}$).

Description of the video file demonstrating automated microextraction

The film can be downloaded from the following URL:

<http://youtu.be/oJ43EMt9Gkc>

The HyperCam software (ver. 2.27, 1996-2012, Hyperionics Technology) was used to record the screens of computers controlling the ion-trap MS and the fluorescence microscope. When the operator presses the “Start” button on the touch screen of the control box, peristaltic pump starts to deliver the extractant (acetonitrile/water = 70:30 (v/v)) to the vial in the extraction chamber. The miniature spindle motor is lowered down by a z-position control mechanism equipped with a stepper motor. Subsequently, a solenoid actuator inserts the inlet section of the sampling capillary to the extraction vial. Both detectors – the fluorescence microscope and the ion-trap MS – record signals during the whole analysis process. Soon after the rotating spindle starts crushing the solid sample, brightness of the recorded fluorescence images (central part of the capillary window) increases, and several signals appear in the recorded mass spectra. When the extraction routine is finished, the miniature spindle motor, and the inlet of the sampling capillary, are moved up so that the sample vial can easily be removed by the operator.

ADDITIONAL TABLES

Table S1. List of the MS signals recorded using the automated microextraction system coupled with ion-trap MS (based on an average mass spectrum from the whole measurement, $S/N > 3$).

Sample	Ion mode	<i>m/z</i> values of detected peaks
Fruit fly	Positive	114.7, 150.7, 168.9, 177.0, 235.4, 247.4, 263.5, 275.6, 279.6, 281.7, 291.7, 303.8, 315.1, 348.0, 360.1, 368.0, 384.0, 446.2, 448.2, 729.8, 731.8, 755.8, 756.8, 757.8, 758.8, 759.8, 760.9, 761.9, 771.9, 773.9, 781.9, 782.8, 783.8, 784.9, 785.9, 786.9
	Negative	<i>cf. Tab. S2</i>
Green tea	Positive	160.0, 166.9, 174.9, 195.0, 201.0, 203.9, 212.9, 261.1, 275.2, 279.1, 381.4, 406.4
	Negative	110.9, 124.9, 136.9, 168.9, 173.0, 179.0, 191.0, 245.1, 261.2, 289.2, 305.2, 351.0, 441.2, 457.2, 471.4, 493.3, 555.4, 649.4, 747.4, 763.4, 795.4, 899.3, 915.3

Table S2. List of the MS signals recorded for fruit fly extract using the automated microextraction system coupled with ion-trap MS and during off-line analysis by electrospray ionization – quadrupole – time-of-flight MS in the negative-ion mode.

Observed <i>m/z</i> (IT)	Observed <i>m/z</i> (Q-TOF)	Putative formula	Predicted <i>m/z</i> [M-H] ⁻	Putative name	Δ <i>m/z</i> (Q-TOF)	MS/MS (Y/N)
123.8	-	unknown	-	unknown	-	N
166.8	-	unknown	-	unknown	-	N
345.9	346.0657	C ₁₀ H ₁₄ N ₅ O ₇ P	346.0558	adenosine monophosphate	0.0099	N
361.9	362.0621	C ₁₀ H ₁₄ N ₅ O ₈ P	362.0507	guanosine monophosphate	0.0114	N
376.0	376.1114	unknown	-	unknown	-	N
392.8	393.0651	unknown	-	unknown	-	N
425.9	426.0368	C ₁₀ H ₁₅ N ₅ O ₁₀ P ₂	426.0221	adenosine diphosphate	0.0147	Y
439.0	439.0980	unknown	-	unknown	-	N
505.9	506.1671	C ₁₀ H ₁₆ N ₅ O ₁₃ P ₃	505.9885	adenosine triphosphate	0.1786	Y
686.4	686.4955	unknown	-	unknown	-	N
688.5	688.5111	unknown	-	unknown	-	N
712.4	712.5092	C ₃₉ H ₇₂ NO ₈ P	712.4923	glycerophosphocholine (31:3) or phosphatidylethanolamine (34:3)	0.0169	N
714.5	714.5244	C ₃₉ H ₇₄ NO ₈ P	714.5079	glycerophosphocholine (31:2) or phosphatidylethanolamine (34:2)	0.0165	N
716.5	716.5379	C ₃₉ H ₇₆ NO ₈ P	716.5236	glycerophosphocholine (31:1) or phosphatidylethanolamine (34:1)	0.0143	N
738.6	738.5256	C ₄₁ H ₇₄ NO ₈ P	738.5079	glycerophosphocholine (33:4) or phosphatidylethanolamine (36:4)	0.0177	N
739.5	739.5289	C ₄₂ H ₇₇ O ₈ P	739.5283	glycerophosphate (39:3)	0.0006	N
740.5	740.5397	C ₄₁ H ₇₆ NO ₈ P	740.5236	glycerophosphocholine (33:3) or phosphatidylethanolamine (36:3)	0.0161	Y
741.5	741.5413	C ₄₂ H ₇₉ O ₈ P	741.5440	glycerophosphate (39:2)	0.0027	N
742.6	742.5501	C ₄₁ H ₇₈ NO ₈ P	742.5392	glycerophosphocholine (33:2) or phosphatidylethanolamine (36:2)	0.0109	N
743.5	743.5255	C ₄₁ H ₇₇ O ₉ P	743.5232	glycerophosphoglycerol (35:2)	0.0023	N
744.4	744.5274	C ₄₀ H ₇₆ NO ₉ P	744.5185	glycerophosphoserine (34:1)	0.0089	N
745.5	745.5218	C ₄₁ H ₇₉ O ₉ P	745.5389	glycerophosphoglycerol (35:1)	0.0171	Y
746.5	746.5248	C ₄₀ H ₇₈ NO ₉ P	746.5341	glycerophosphoserine (34:0)	0.0093	N
771.4	771.5360	C ₄₂ H ₇₇ O ₁₀ P	771.5182	glycerophosphoglycerol (36:3)	0.0178	N
784.5	784.5284	C ₄₂ H ₇₆ NO ₁₀ P	784.5296	glycerophosphoserine (36:3)	0.0012	Y
786.5	786.5443	C ₄₂ H ₇₈ NO ₁₀ P	786.5291	glycerophosphoserine (36:2)	0.0152	Y

831.5	831.5251	C ₄₃ H ₇₇ O ₁₃ P	831.5160	glycerophosphoinositol (34:3)	0.0091	N
832.5	832.5286	C ₄₆ H ₇₆ NO ₁₀ P	832.5134	glycerophosphoserine (40:7)	0.0152	N
833.5	833.5388	C ₄₄ H ₈₃ O ₁₂ P	833.5549	glycerophosphoinositol (34:2)	0.0161	Y
834.5	834.5417	C ₄₆ H ₇₈ NO ₁₀ P	834.5291	glycerophosphoserine (40:6)	0.0126	N
835.5	835.5495	C ₄₃ H ₈₁ O ₁₃ P	835.5342	glycerophosphoinositol (34:1)	0.0153	Y
857.5	857.5389	C ₄₅ H ₇₉ O ₁₃ P	857.5186	glycerophosphoinositol (36:4)	0.0203	Y
858.6	858.5420	C ₄₈ H ₇₈ NO ₁₀ P	858.5291	glycerophosphoserine (42:8)	0.0129	N
859.5	859.5536	C ₄₅ H ₈₁ O ₁₃ P	859.5706	glycerophosphoinositol (36:3)	0.0170	Y
860.5	860.5574	C ₄₈ H ₈₀ NO ₁₀ P	860.5447	glycerophosphoserine (42:7)	0.0127	N
861.5	861.5653	C ₄₅ H ₈₃ O ₁₃ P	861.5499	glycerophosphoinositol (36:2)	0.0154	N

ADDITIONAL FIGURES

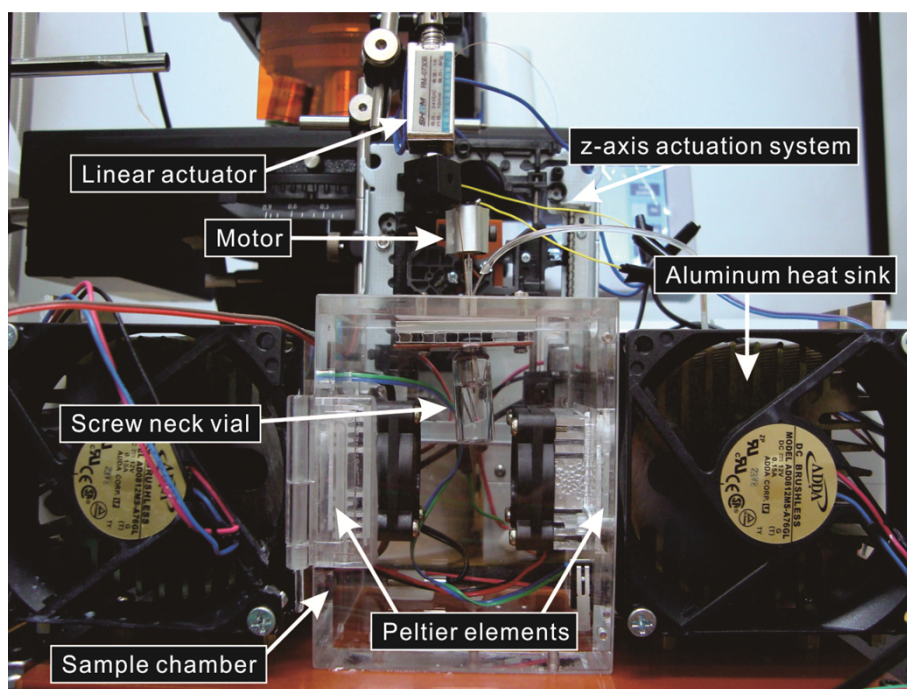


Fig. S1 Photograph of the sample microextraction device.

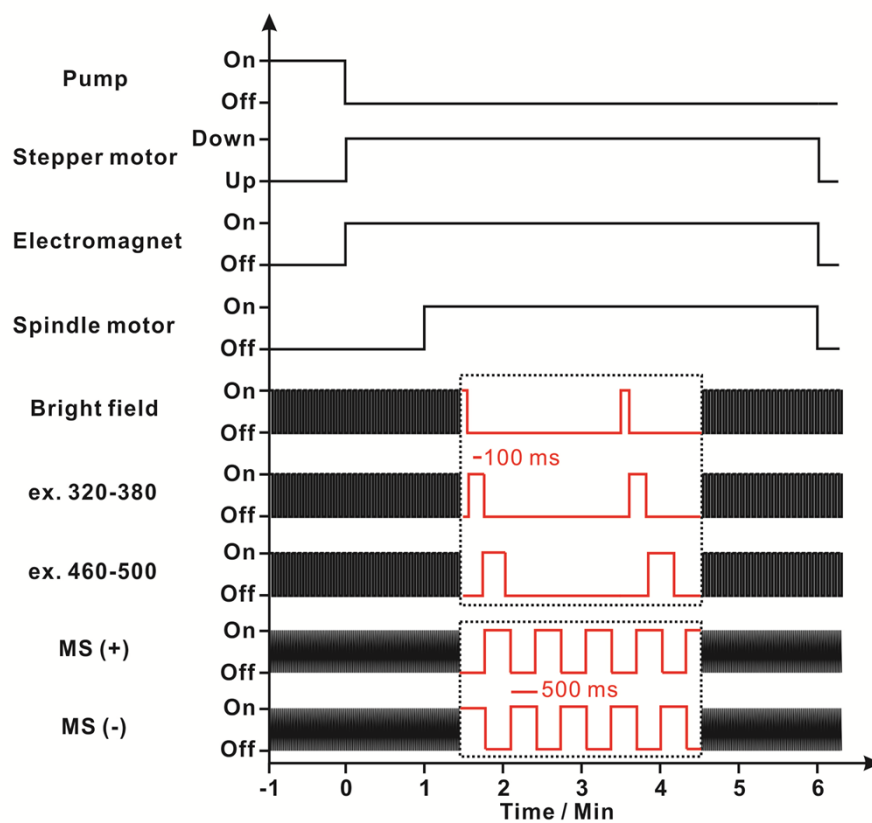


Fig. S2 Duty cycles of various functions incorporated into the automated microextraction system. The dashed frame contains an expansion of the duty cycle lines for better clarity.

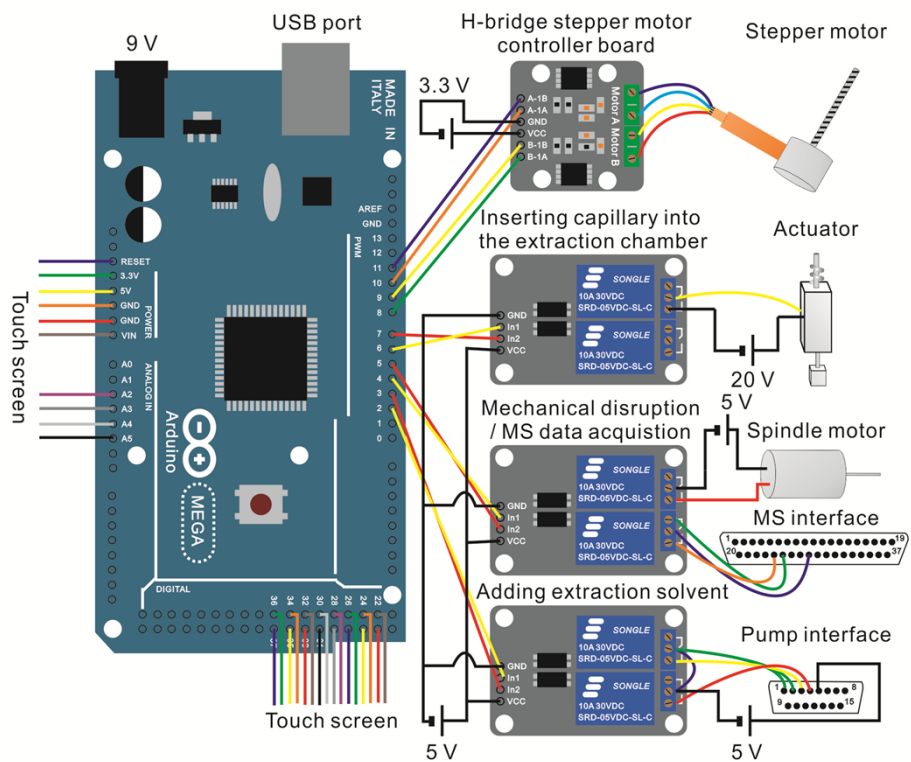


Fig. S3 Schematic representation of the electronic device used to control the microextraction system. The device incorporates an Arduino Mega PCB and several auxiliary PCBs.

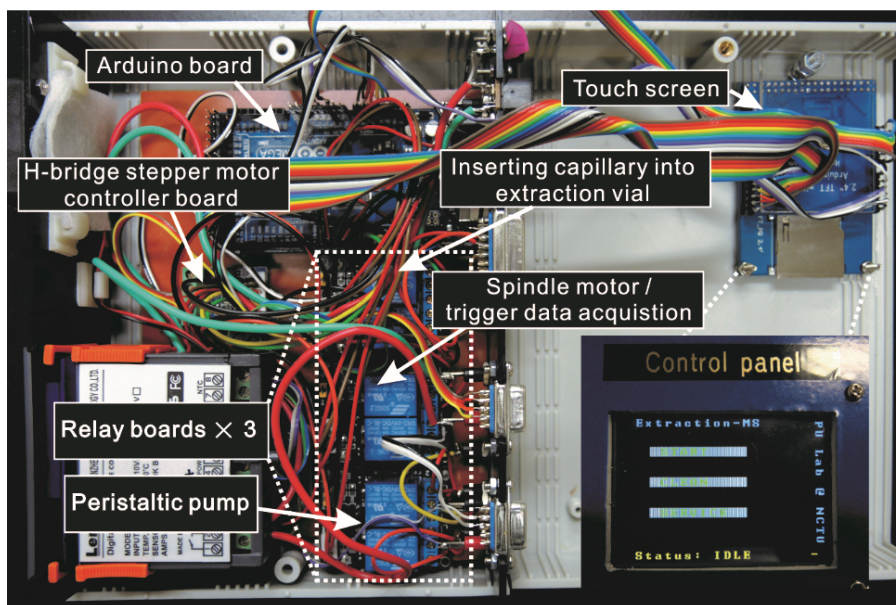


Fig. S4 Photograph of the electronic device used to control the microextraction system (disassembled, inside view). The inset shows the front of the device (touch screen).

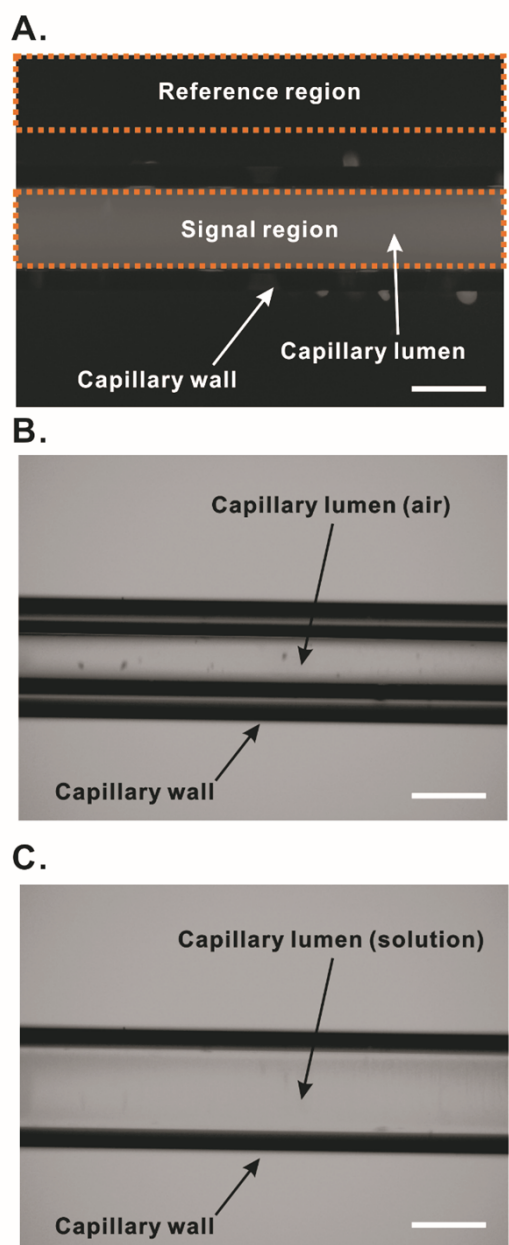


Fig. S5 Images of the sampling capillary captured by the microscope incorporated in the experimental system: (A) Fused silica capillary imaged by the fluorescence microscope ($\lambda_{\text{ex}} = 320\text{-}380$ nm). Signal and reference regions of the image are indicated (see Experimental section for details). (B) Empty capillary (bright field mode). (C) Sample solution inside the capillary (bright field mode). Scale bars: 150 μm .

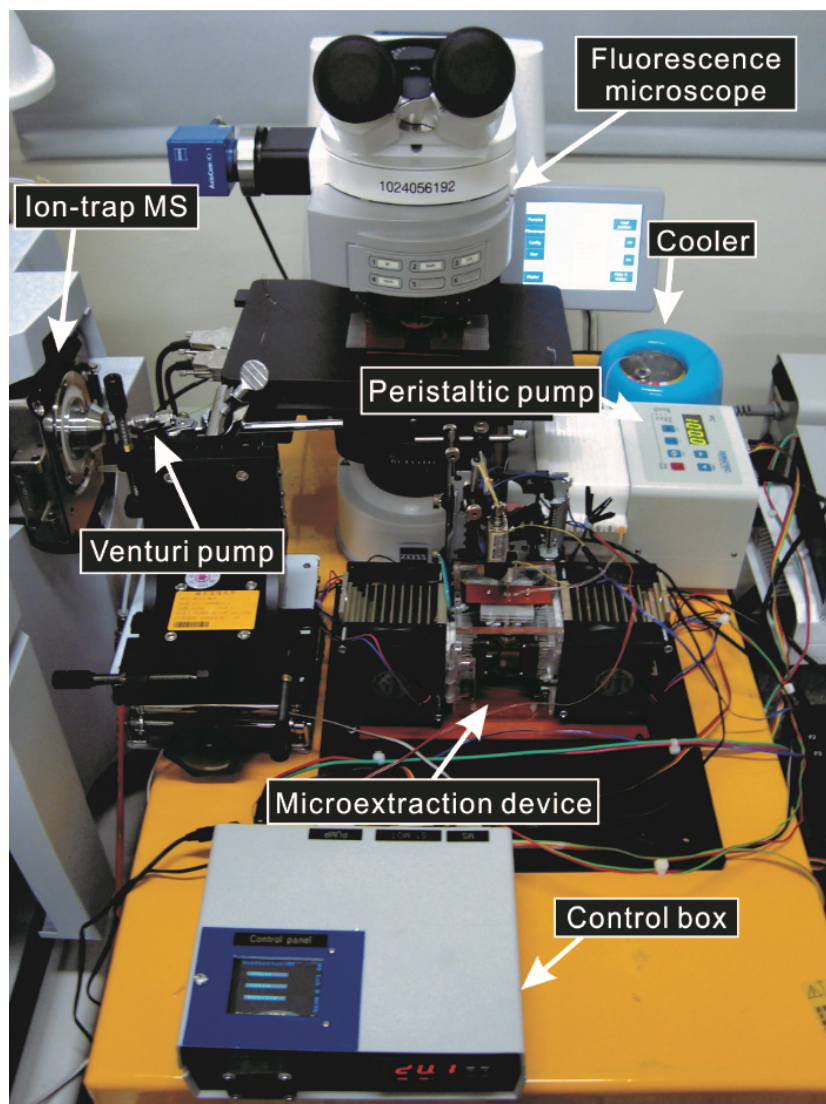


Fig. S6 Photograph of the entire experimental setup.

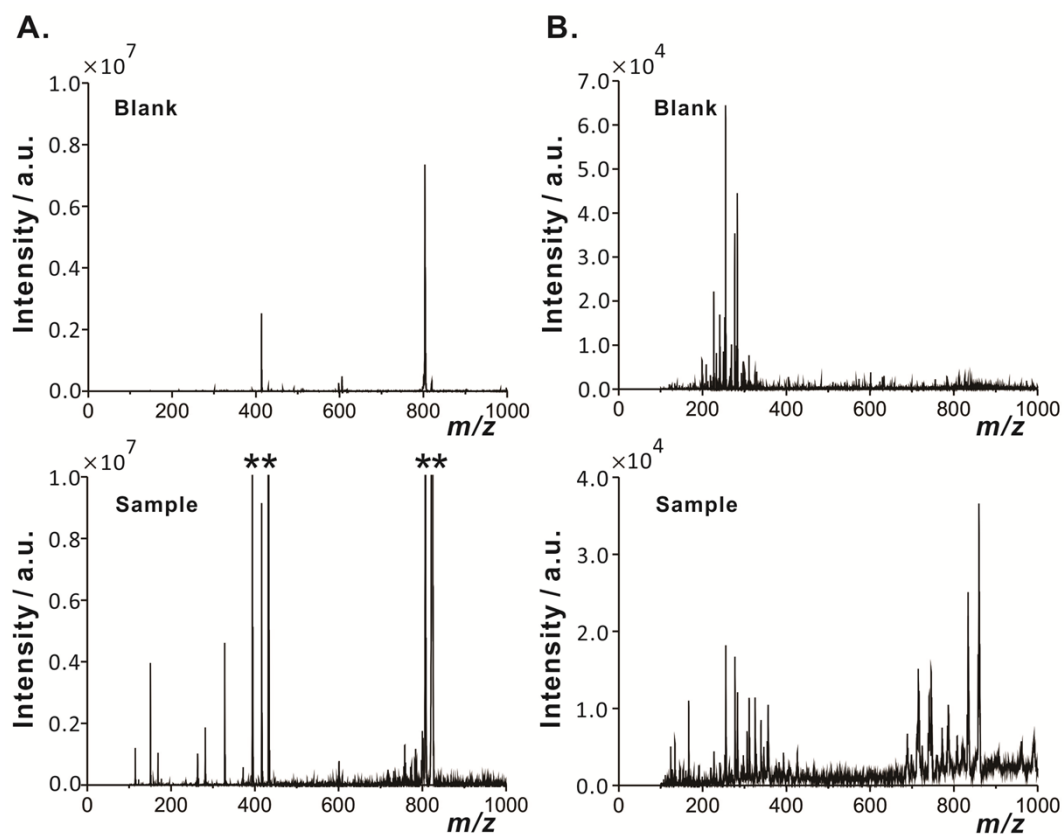


Fig. S7 Mass spectra of a female fruit fly specimen obtained by the automated microextraction system coupled with MS: (A) Blank spectrum (top) and sample spectrum (bottom) in positive-ion mode; (B) Blank spectrum (top) and sample spectrum (bottom) in negative-ion mode. Asterisks (*) indicate the peaks which are higher than the vertical axis range.

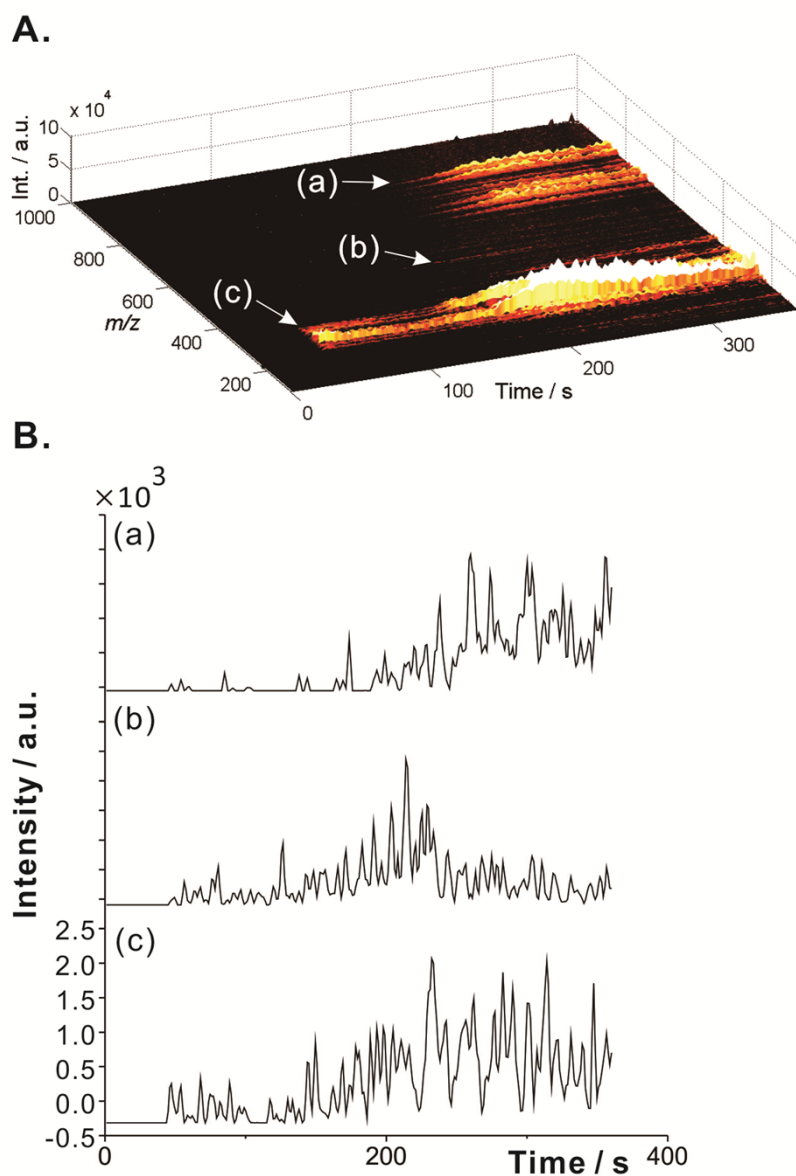


Fig. S8 Negative-ion mode time-resolved MS record of the extraction of a single fruit fly sample using the automated system. The background (average spectrum from the early stage of extraction of 50 s to 60 s) has been subtracted. (A) Three-dimensional plot; (B) (a) m/z 860; (b) m/z 518; (c) m/z 329.

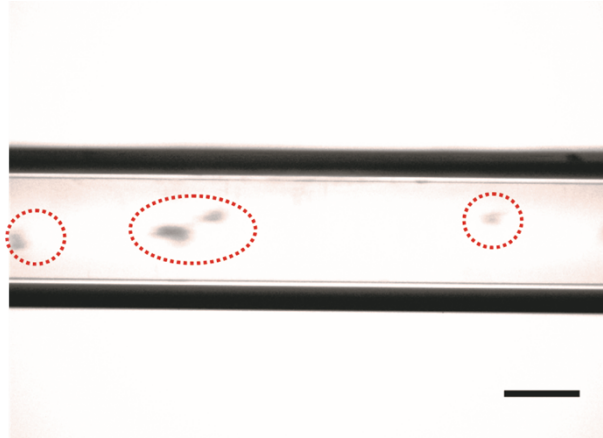


Fig. S9 Image of the sampling capillary taken by the upright microscope (brightfield mode). In this snapshot, small particles of a disrupted fruit fly specimen (aspirated by the sampling capillary) pass the detection window (indicated with red dotted lines). Scale bar: 150 μm .

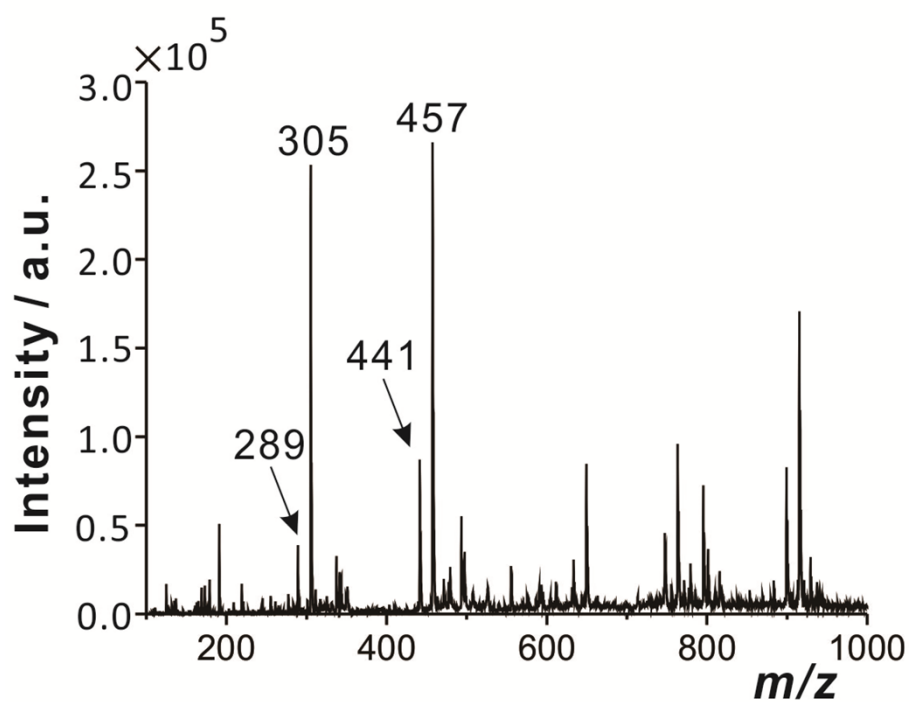


Fig. S10 Negative-ion mode mass spectrum of a fragment of green tea leaf obtained by the automated microextraction system coupled with MS (average spectrum at the 6th minute of analysis). The signals at the m/z values 289, 305, 441, and 457, correspond to catechin or epicatechin; gallocatechin; epicatechin 3-gallate or catechin 3-gallate; epigallocatechin 3-gallate or gallocatechin 3-gallate, respectively.

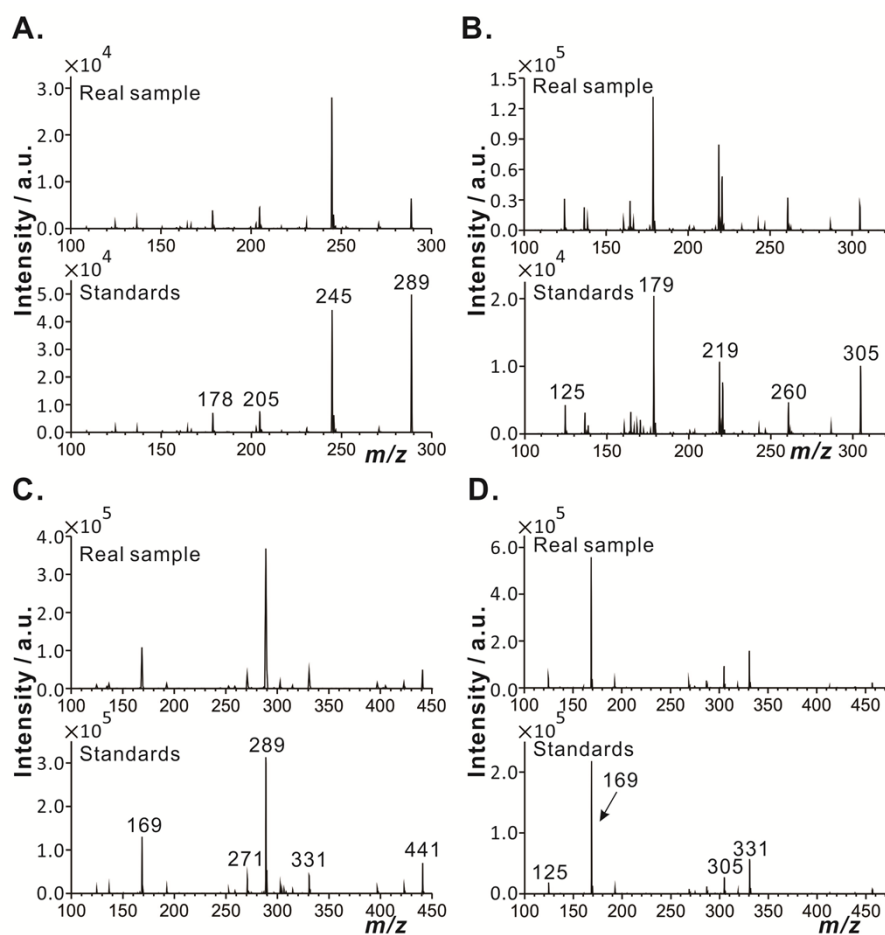


Fig. S11 Negative-ion mode tandem mass spectra of the extract from green tea leaves and a green tea catechin mix standard mixture (concentration $\sim 10^{-5}$ M in acetonitrile/water = 80:20 (v/v); purchased from Cerilliant, Round Rock, TX, USA) analyzed by electrospray ionization – ion-trap MS. Signals of the precursor ions at the m/z (A) 289, (B) 305, (C) 441 and (D) 457 are characteristic of catechin or epicatechin; galocatechin; epicatechin 3-gallate or catechin 3-gallate; epigallocatechin 3-gallate or galocatechin 3-gallate, respectively.